Available online at www.sciencedirect.com
ScienceDirect
Carbohydrate Polymers 69 (2007) 503–511
Carbohydrate Polymers
www.elsevier.com/locate/carbpol

Addition of glycerol plasticizer to seaweeds derived alginates: Influence of microstructure on chemical–physical properties

Maurizio Avella [a], Emilia Di Pace [a], Barbara Immirzi [a], Giuseppe Impallomeni [b], Mario Malinconico [a], Gabriella Santagata [a,*]

[a] *Institute of Chemistry and Technology on Polymers, National Research Council, Via Campi Flegrei, 34 – 80078 Pozzuoli (Na), Italy*
[b] *Institute of Chemistry and Technology on Polymers, National Research Council, Viale A. Doria, 6 – 95125 Catania, Italy*

Received 1 December 2006; received in revised form 5 January 2007; accepted 8 January 2007
Available online 25 January 2007

Abstract

A study of the interaction among sodium alginates of different molecular compositions, water and glycerol was carried out, in order to weigh up the influence of different polymeric microstructures on the chemical–physical properties of films obtained by water soluble blends of sodium alginates and increasing amounts of glycerol. Thermal, mechanical and morphological analyses performed on the films confirmed the existence of specific interactions between sodium alginates and glycerol; it was as well demonstrated that only at specific mass ratio between the single polymers and glycerol it is possible to obtain the correct plasticizing effect induced by glycerol.

Keywords: Alginate; Glycerol; Microstructure; Thermal and mechanical characterizations

1. Introduction

Algin, the common definition used to specify the salts of alginic acid, takes place in all the members of the Phaeophyceae, a class of brown seaweeds, in which alginic acid represents the structural component of intercellular walls, providing both strength and flexibility to the algal tissue.

It exists in the form of insoluble gel of mixed calcium, magnesium, sodium and potassium salts, and it is extracted from the grounded thallium upon the collapse and subsequent transformation of their tissue in a brown mass (Draget, Smidsrød, & Skjak-Braek, 2002; Fischer & Dorfel, 1955). The alginic acid is a complex mixture of oligo-polymers, polymannuronic acid (MM), polyguluronic acid (GG) and a mixed polymer (MG) where sequences like GGM and MMG co-exist too (Atkins, Nieduszynsky, Parker, & Smolko, 1973a,b; Haug, Larsen, & Smidsrod, 1966; Smidsrod, Haug, & Larsen, 1966). The mannuronic acid forms β (1–4) linkage, so that M-block segments show linear and flexible conformation; the guluronic acid, differently, gives rise to α (1–4) linkage, introducing in this way a steric hindrance around the carboxyl groups; for this reason the G-block segments provides folded and rigid structural conformations, responsible of a pronounced stiffness of the molecular chains. In Fig. 1 the M and G blocks of the alginic acid salts with their sequence are reported.

In water solution and in the presence of divalent cations such as calcium ion, the peculiar buckled backbone of G segments gives rise to water insoluble gels due to the strong interaction between the divalent cations and the COO– groups of the base residual of guluronic acid; they can trap the cations in a stable, continuous and thermo-irreversible three-dimensional network, whose conformation is typical of an *egg box* as shown in Fig. 2 (Grant, Morris, Rees, Smith, & Thom, 1973; Grasdalen, Larsen, & Smidrod, 1981). The earlier statements reflect in the enormous applicative versatility of the polymer, strictly dependent on the guluronate residues content (M/G), on the sequential structure ($F_G, F_M, F_{GG}, F_{MG}, F_{GM}$), on the average number of

* Corresponding author. Tel.: +39 0818675212; fax: +39 0818675230.
E-mail address: santagata@ictp.cnr.it (G. Santagata).

0144-8617/$ - see front matter © 2007 Published by Elsevier Ltd.
doi:10.1016/j.carbpol.2007.01.011

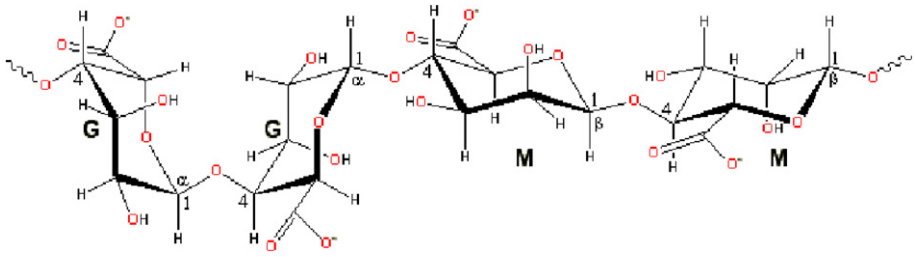

Fig. 1. Sodium alginate molecular structure.

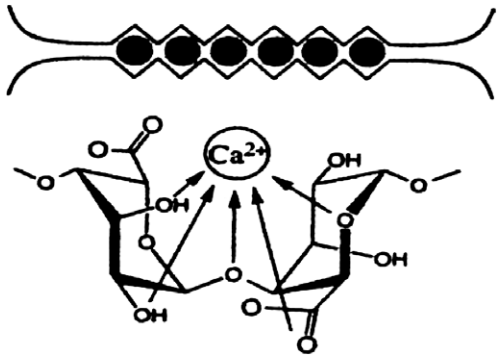

Fig. 2. "Egg-Box" structure.

consecutive guluronate moieties in G-blocks structures ($N_{G>1}$) and on the molecular mass distribution (M_W, M_N, P.I).

The microstructural features of sodium salts of alginic acid reflects in their ability to show gelling and stabilizing properties widely used in important applications such as medicine, drug transport, controlled release, immobilization of herbicides and micro-organisms, as well as in food applications, where the polysaccharide plays an important role as phytocolloid as well as an emulsifying agent (Atkins, 1985; Clark & Ross-Murphy, 1987). In previous studies carried out at our Institute, biodegradable films based on natural as well as synthetic polymers, by water casting methodologies, have been obtained and characterized (De Prisco et al., 2002; Immirzi, Malinconico, Romano, Russo, & Santagata, 2003; Russo, Giuliani, Immirzi, Malinconico, & Romano, 2004; Russo, Malinconico, Petti, & Romano, 2005). A possible applicative target of such water-cast films is in protected cultivation, i.e. realization of mulching film. As concerning the use of biodegradable films in agriculture, recently fundamental studies have been carried out and complete coverage is found in literature. In particular, the achievements and the problematics relative to the performance of thermoplasticized starch based films (Mater-Bi) tested on the soil and compared to petroleum derived plastic films (Briassoulis, 2006a – Polymer degradation and stability; Briassoulis, 2006b – Journal of polymers and the environment) are described. With the aim to go into this topic, the attention of the following paper is centred on the study of the interactions between sodium alginates and natural plasticizers. We plan to study the chemical–physical properties of biodegradable films obtained by water blending and casting sodium alginates with increasing amounts of glycerol plasticizer. Two alginates with different molecular weights and different M/G ratios have been used and mechanical, thermal and morphological properties of the films performed have been studied. The future target of our study consists in spraying the water solution of polymeric blends on the soil, in this way producing a protective thin membrane (a sort of varnishes) that cover the soil (Schettini, Vox, Malinconico, Immirzi, & Santagata, 2005).

The spray methodology could represent an absolute innovative practice to prepare films for agriculture.

2. Experimental

2.1. Materials and films achievement

Sodium alginate (NaAlg) was kindly supplied by FMC BioPolymer, Belgium. Two types of alginate were used: one of high guluronic acid content (Protonal LF 20 alginate with the identification code "Ap") ($M_w = 1.08 \times 10^6$ Da, M_n (1.98×10^5 Da, $P = 5.5$) and one of low guluronic acid content (Scogin LV alginate with the identification code "Ar") ($M_w = 5.86 \times 10^5$ Da, $M_n = 1.14 \times 10^5$ Da, $P = 5.1$), as given by the manufacturer.

Glycerol was provided by Fluka and used as received. Films are obtained through water solution casting. In all samples, 2 g of NaAlg and 200 mL of water are put in a conical flask equipped with a reflux condenser. The system is taken to 70–75 °C under mechanical stirring. After dissolution different amounts of glycerol are added, in order to achieve four compositions of NaAlg/Gly wt/wt for each polymeric matrix used. Each final solution is then transferred on a PMMA surface of 20 cm^2 and air dried for 48 h, to get a regular detachable film. The thickness of films are in the range between 40 and 50 μm. Before testing the films are equilibrated at 48% RH by putting them in desiccators over saturated calcium nitrate tetrahydrate solution.

The obtained films of neat alginates are essentially amorphous as revealed by X-ray diffraction analysis (not reported). The addition of plasticizer seems to increase the level of "amorphicity" of the films, although a more detailed analysis of diffraction pattern will be subject of further investigations.

The compositions of the blends with their identification codes are reported in Table 1.

Table 1
Composition of binary Ap-based blends and Ar-based blends

Sample	Code	% NaAlg (wt)	% Glycerol (wt)
NaAlg	Ap	100	0
NaAlg/glycerol	ApG1	67	33
NaAlg/glycerol	ApG2	55	45
NaAlg/glycerol	ApG3	50	50
NaAlg	Ar	100	0
NaAlg/glycerol	ArG1	67	33
NaAlg/glycerol	ArG2	55	45
NaAlg/glycerol	ArG3	50	50

2.2. Characterization and testing

2.2.1. Nuclear magnetic resonance (NMR)

Chemical composition and sequential structure of alginate can be determined by ^{1}H NMR spectroscopy. The NMR methodology and assignments are based on data published by Grasdalen, Larsen, & Smidrod (1979, 1981, 1983) Heyraud, Leonard, Rochas, Girond, & Kloareg (1996). The characterization was performed using a 500 MHz Varian Unity INOVA spectrometer. The spectra were collected at 50 °C following the Standard Test Method F 2259-03.

2.2.2. Size exclusion chromatography (SEC)

The average molecular weights, M_w, and the distribution of the molecular weights in the alginate samples were determined by size exclusion chromatography. Three columns, HB 40, HB 1000 and HB 40 from PSS Mainz, a detector Shodex RI 71, Fa. Showa Denko, a SP Thermo Separation Products pump (TSP) were used.

The calibration was performed using dextran, the eluent was a 0.1 M solution of $NaNO_3$ at a flow rate of 1 ml/min.

2.2.3. Differential scanning calorimetry (DSC)

Thermal analyses were carried out using a Mettler DSC 30 calorimeter coupled to a Mettler TC10A/TC15 processor. The apparatus was calibrated with pure indium, lead and zinc standards at various scanning rate. Dry nitrogen gas with a flow rate of 20 ml/min was purged through the cell during all measurements and thermal treatments. Samples were subjected to a thermal cycle over the temperature range of −100 to 250 °C in an inert atmosphere of liquid nitrogen. Runs were conducted on samples of about 9 mg at the heating rate of 10 °C/min.

2.2.4. Dynamical mechanical thermal analysis (DMTA)

Thermal analyses were performed by using the MKIII equipment of Scientific Rheometric. Measurements were obtained on parallelepiped-shaped specimens of 1 mm × 15 mm × 20 mm. The amplitude of the oscillation was set at 16 μm; the range of temperature chosen was between −100 and 200 °C, the experiment were performed under nitrogen with the heating rate of 5 °C/min and 1 Hz of frequency.

2.2.5. Mechanical properties

Young's modulus, stress and strain at break data were obtained on a PC assisted dynamometer Instron Mod.4301, which conforms to the ISO 5893 standard.

For mechanical tests dumbbell specimens by a width of 1 cm, a length of 4 cm and a thickness of 40–50 μm were used. For each composition six specimens were tested. All the measurements were carried out at room temperature, at crosshead rate of 2 mm min^{-1}, at gauge length of 22 cm and at nominal strain rate of 0.45 min^{-1}.

2.2.6. Scanning electron microscopy (SEM)

Morphological analysis was carried out by Scanning Electron Microscopy using a Philips XL 20 series microscope on cryogenically fractured surfaces. Before the electron microscopy observation, the fractured surfaces were coated with Au–Pd alloy with a SEM coating device (SEM BALTEC MED 020). The coating provides the entire sample surfaces with a homogeneous layer of the metal of 18 ± 0.2 nm.

3. Results and discussion

3.1. Neat polymers (Ap and Ar)

3.1.1. Nuclear magnetic resonance (NMR) spectroscopy

In Table 2 the guluronic and mannuronic acids content (F_G, F_M), and the average number of consecutive guluronate moieties in G-block structures are detailed.

In Figs. 3 and 4 the NMR spectra of Ap (Fig. 3) and of Ar (Fig. 4) polymers are reported.

NMR spectrum of Ar polymer (Fig. 4) shows the typical peaks of alginic acid (Heyraud et al., 1996). Besides, as concerning NMR spectrum of Ap polymer (Fig. 3), in addition to the usual signals of alginic acid, some peaks not characteristic of the polysaccharide have been observed. They may be ascribed to components of lower molecular weights such as saccharose.

3.2. Thermal properties

In Fig. 5 (curve Ap) and Fig. 6 (curve Ar), the results of DSC analysis of the two neat polymers are reported.

The DSC curves show both the endothermic peaks due to the water releasing of the two systems for the different compositions, and the exothermic peaks due to polymer degradation. From literature data (Haly & Snaith, 1971), it is possible to discriminate four different kinds of water, from the strongly bound water to the completely free one.

Table 2
NMR data of Ap and Ar polymers

Sample	F_G (%)	F_M (%)	$N_{G>1}$ (%)
Ap alginate	61 ± 0.1	39 ± 0.1	6.8 ± 10
Ar alginate	45 ± 0.1	55 ± 0.1	3.3 ± 10

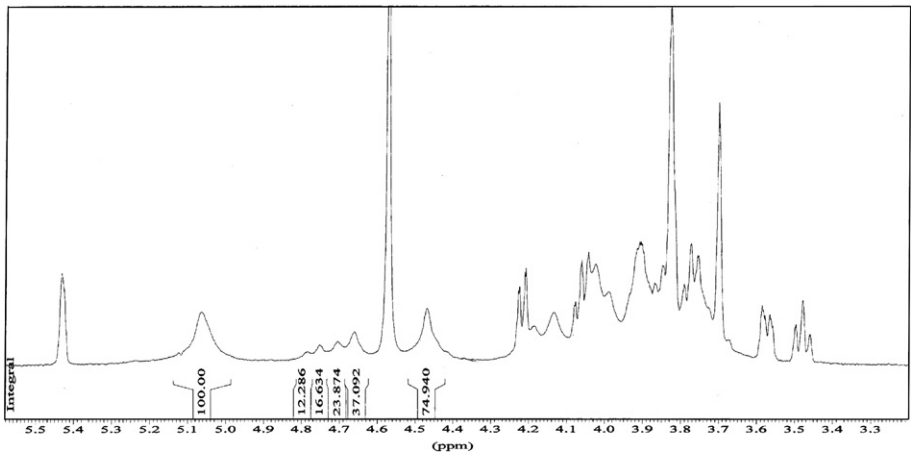

Fig. 3. NMR spectrum of Ap.

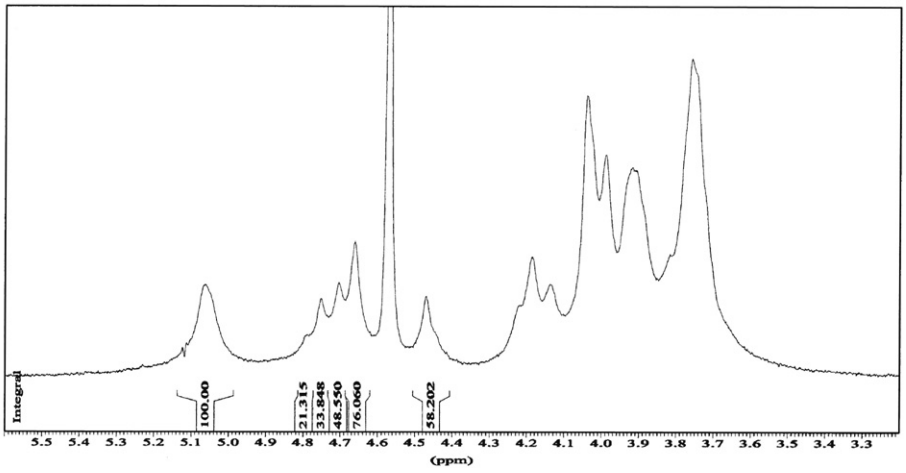

Fig. 4. NMR spectrum of Ar.

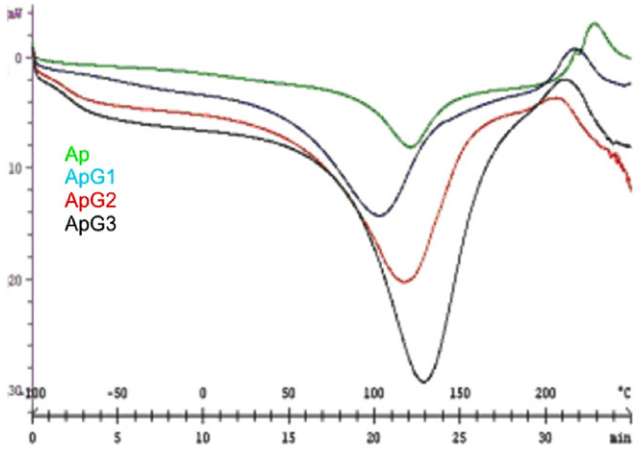

Fig. 5. DSC curves of Ap system.

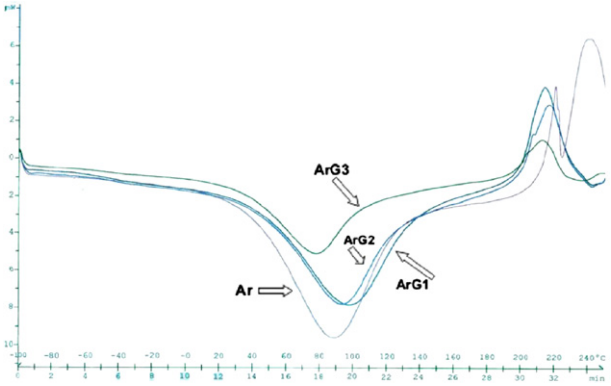

Fig. 6. DSC curves of Ar system.

As concerning alginates, it is possible to propose the existence of three different kinds of water: the first one is free water and it is released in the range 40–60 °C, the second one, bound to the –OH groups (dipole–dipole interaction), is discharged until 120 °C and the third one, linked to the $–COO^-$ groups (ion–dipole interaction) is released until 160 °C. The stronger ion–dipole bond strength explains the higher temperature necessary for the evolution of the third kind of water (Seon, Seoung, & Sun, 2003).

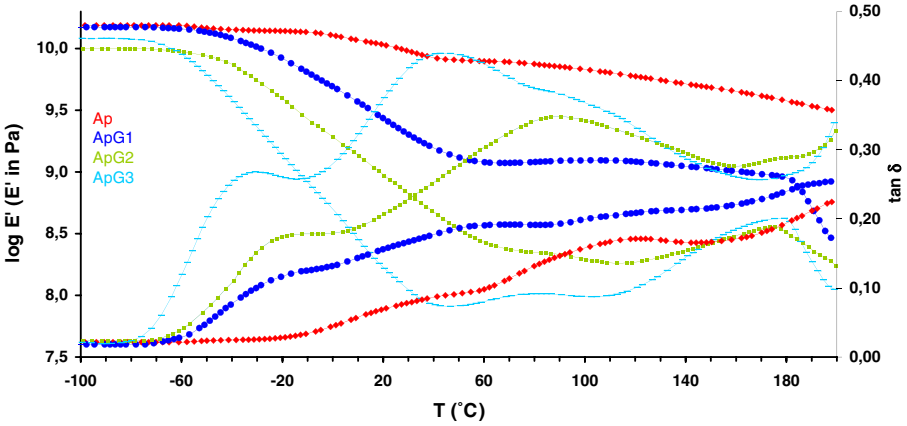

Fig. 7. DMTA curves of Ap system.

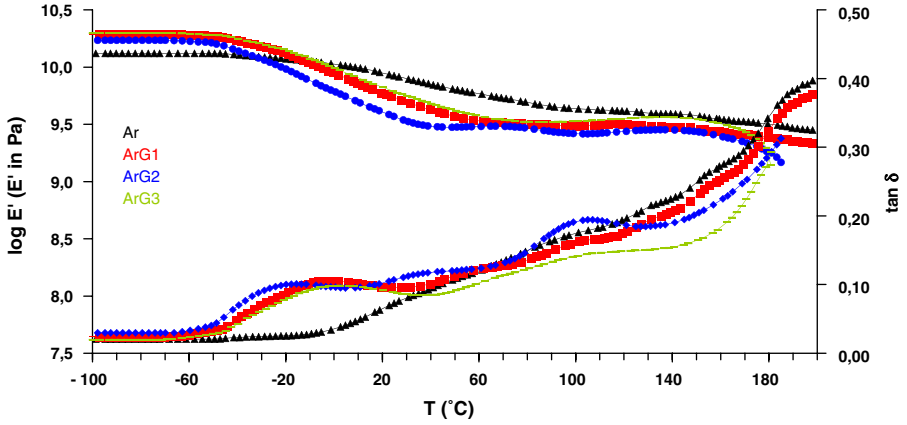

Fig. 8. DMTA curves of Ar system.

As far as our blends, in all the curves it is possible to note that significant amounts of weakly bound water starts to be released at about 40 °C (Borchard, Kenning, Kapp, & Mayer, 2005; Nakamura, Nishimura, Hatakeyama, & Hatakeyama, 1995; Seon et al., 2003) while the evolution of the water trapped in hydrogen bonding with the components of the blends occurs at higher temperatures, according to the different compositions. Moreover, by the analysis of 100% sodium alginates curves, (Figs. 5 and 6), it can be observed that maximum values relative to the water releasing peaks are at about 130 °C for Ap polymer and at about 90 °C for Ar polymer; this considerable difference in temperature values for the two polymers is firstly due to the dissimilar physical hindrances for bound water to be evaporated (Haly & Snaith, 1971).

Particularly in the case of Ap alginate, it is possible to evidence that the water is strongly retained with respect to Ar polymer; this behaviour can be ascribed to the following reasons: higher molecular weight of the polymer, which is responsible of a stiff and strong network, the larger amount of guluronic residues liable of a folded molecular structure and the longer guluronate segments in G blocks, accountable of a better-organized association of molecular chains (Ap-N_G > Ar-N_G, Table 2).

These considerations are also confirmed by DMTA results. In Fig. 7-Ap and in Fig. 8-Ar the DMTA curves for the two systems are reported The Ap and Ar DMTA curves show a similar profile until about 40 °C (releasing of weakly bound water); above this temperature, the alginates–water interactions of the two systems change. In Ap system, the strong interaction between polymer and water gives rise to a plasticizing plateau in the range of 40–80 °C; above this temperature, the elastic modulus regularly falls down and the loss factor, $\tan\delta$, assumes a maximum value around 120 °C, in correspondence of Ap glass transition temperature.

In Ar polymer $\log E'$ regularly decreases in the range of temperature considered (40–80 °C) in agreement with the weaker interaction alginate-water, while $\tan\delta$ shows the loss peak relative to glass transition temperature at about 100 °C.

3.3. Mechanical properties

In Table 3 the mechanical properties of the neat polymers are reported.

Comparing the Young's modulus values of the two polymers, it is possible to observe that, in opposition to the expected result, the polymer with the higher amount of guluronic acid (Ap) shows the lower value.

This outcome is probably due to the slight plasticizing effect induced by the presence of polymeric components of

lower molecular weight as revealed by results of NMR analysis for Ap alginate.

On the other hand, the higher amount of guluronic acid (61%), indicative of a folded and stiffer molecular structure, is responsible of a lower value in elongation at break (see Table 3).

3.4. Scanning electron microscopy (SEM) properties

Following the micrographs of Ap (Fig. 9) and Ar (Fig. 10) surfaces fractured in liquid nitrogen are reported.

From Fig. 9 (Ap) it is possible to evidence both a smooth surface, typical of a soft polymer (as confirmed by mechanical properties) and some irregularities spread on the surface, probably belonging to foreign materials (as evidenced by NMR analysis).

From Fig. 10 (Ar) the rigid fracture surfaces is characteristic of a stiff polymer. Once again, this confirms the obtained mechanical properties.

Table 3
Mechanical properties of Ap and Ar polymers, Ap-based blends and Ar-based blends (film thickness = 40–50 μm)

Sample	Young's modulus (MPa) ± 10%	Stress at break (MPa) σ_b ± 20%	Strain at break (%) ε_b ± 10%
Ap	2326	44.9	2.13
Ar	3456	82.7	3.75
ApG1	431	20.1	9.4
ApG2	74	6.0	17.7
ApG3	17	5.3	32.2
ArG1	1135	21.93	4.88
ArG2	1054	21.11	5.05
ArG3	626.4	18.0	8.70

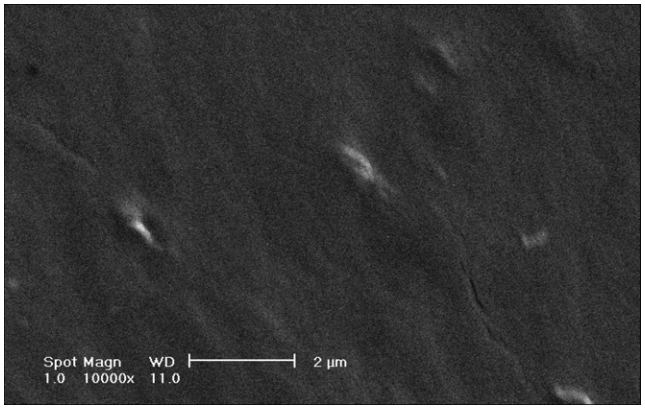

Fig. 9. SEM micrograph of Ap sample fracture surface.

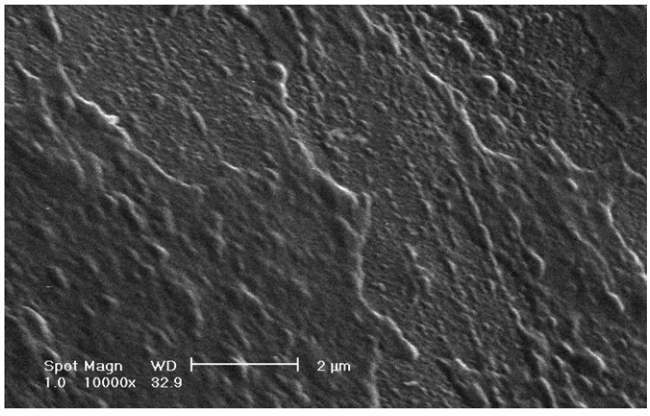

Fig. 10. SEM micrograph of Ar sample fracture surface.

3.5. Plasticized polymers: ApG

3.5.1. Thermal analysis (DSC and DMTA)

The DSC thermograms relative to ApG blends (Fig. 5) show, as observed in the case of the neat polymer, the presence of the endothermic peaks corresponding to the water losses from the different blends. From the analysis of ApG1 curve it is clear that the peak position of water releasing temperature decreases of about 20 °C with respect to the neat polymer, moving from 130 to 110 °C. This effect may be due to a preferential interaction between glycerol and alginate, which expels water from the structure. Hence, water is released at lower temperature. On the contrary, the endothermic peaks relative to the water losses from ApG2 and ApG3 blends are broader and shifted again towards higher temperatures, respectively 120 and 130 °C. This result seems to indicate the presence of glycerol exceeding the amount accepted by the alginate polymer. This excess glycerol then interacts with water, and as consequence bound water is released at higher temperature.

By the analysis of DMTA curves (Fig. 7), the glass transition temperature T_g (maxima of $\tan\delta$) and the elastic modulus ($\log E'$) are observable for the different blends. In ApG1 blend, $\log E'$ starts regularly decreasing in correspondence with the glycerol T_g occurring at about −20 °C; in the range 60–110 °C a plasticizing plateau is noticeable according to a stable structural interactions between the polymer and the glycerol; in the same range two different transitions can be distinguished by $\tan\delta$: the first one at 60 °C due to the development of weakly bound water and the second one, at about 120 °C, corresponding to the polymer T_g.

In the case of ApG2 blend, the polymer T_g is centred at about 90 °C and the glycerol T_g is slightly shifted to lower temperature; in the case of ApG3 blend, in addition to the T_g of glycerol (shifted at −30 °C), two transitions are observable too: the first one at 50 °C due to the developing of weakly bound water and the second one, at 90 °C, corresponding to the polymer T_g.

3.6. Plasticized polymers: ArG

3.6.1. Thermal analysis (DSC and DMTA)

From the analysis of DSC curves of ArG system (Fig. 6) the endothermic peaks due to the water developments are observable. The endothermic peak of neat polymer occurs at 90 °C, whereas ArG1 and ArG2 blends show the endothermic peaks at about 100 °C. In the case of ArG3 composition, instead, it is possible to detect the peak maximum corresponding to the water releasing temperature at 80 °C.

From the above, it is possible to affirm that a clear plasticizing effect of glycerol is only observed for the ApG3 blend.

The DMTA curves of ArG1 and ArG2 systems show similar thermal profile: in correspondence to the glycerol T_g, showed by a maxima of $\tan\delta$ at −10 °C, $\log E'$ regularly falls down until 60 °C, temperature at which a first transition due to the weakly bound water evolution occurs. The glass transition temperatures of the polymer are showed by two shoulders of $\tan\delta$ occurring at about 100 °C. The DMTA curve of ArG3 blend shows the glycerol T_g shifted to −20 °C, a first transition visible at 40 °C due to the weakly bound water releasing and a second well discernible transition at 100 °C ascribed to the polymer T_g.

Thermal analysis performed on ArG system suggests that the molecular network of the polymer does not appreciably change with respect to the introduction of increasing amounts of glycerol for the first two blends (33% and 45% of plasticizer); it is possible to emphasize that only in ArG3 blend an early plasticizing effect may be pointed out: the glass transition of the glycerol and the development of free water are recorded at lower temperatures with respect to ArG1 and ArG2 compositions.

3.7. Comparison between thermal properties of ApG and ArG systems with respect to the different microstructures

The different thermal performance of the two neat polymers and of the blends suggests the hypothesis of a strict correlation between the observed properties and the polymeric microstructures.

Comparing DSC curves of Ap and Ar systems, it finds out that the endothermic peaks related to maxima water losses are located at different range of temperatures; in fact for Ar system the temperature range is 80–100 °C, while the interval for Ap system is 110–130 °C.

Comparing DMTA curves of Ap and Ar based systems, it is evident the diverse plasticizing action of glycerol on polymeric matrixes; in ApG2 and ApG3 blends, the excess of plasticizer provides a drastic drop of modulus and a decreasing of polymer T_g, while in Ar system only the ArG3 blend shows an early plasticizing effect.

The different thermal behaviours could be explained on the base of the microstructural features of Ap and Ar polymers.

In Ap polymer the higher value of M_w is indicative of a longer average chain length, and the higher fraction of guluronic acid is accountable of a buckled and folded structure in which a plasticizer is probably entrapped quite firmly; in fact, the addition of 33% of glycerol causes a clear plasticizing effect of the polymer, as shown by the DSC and the $\log E'$ curves (Figs. 5 and 7). Because of this stronger interaction, the water can release the polymeric binding sites at lower temperatures (Fig. 5) with respect to the neat polymer. On the other hand, DSC curves of ApG2 and ApG3 blends evidence a rising of water evolution temperature (Fig. 5); this occurrence seems to indicate that at 33% glycerol content the accessible interactive sites of the polymer have been already saturated and increased amounts only goes to interact with water.

In Ar polymer, the lower value of M_w is indicative of shorter average chain length and the higher fraction of mannuronic acid accounts of a greater overall flexibility. In this network the water is not strongly retained; in fact, evaluating the ranges of temperature in which the endothermic peaks of Ap and Ar systems occur, (Figs. 5 and 6), it is possible to note a shift towards lower values of water evolution temperature for Ar system.

On the other side, the intermolecular interaction polymer–water is such as to hamper the plasticizing effect of the glycerol until a specific concentration is not achieved; in fact only when 50% of glycerol is added to the polymer, a slight plasticization may be observed.

3.8. Mechanical properties

In Table 3 the mechanical properties of ApG and ArG blends are reported.

Both the systems show a decreasing of Young's modulus going from the neat polymer to the blends. In Ap system, moving from ApG1 to the other blends, a notable drop in the elastic modulus and stress at break are detected. Such a result may be attributed to the excessive amounts of glycerol introduced in the blends and to the resulting change of chemical interactions among polymer, glycerol and water as discussed before.

In Ar system, passing by the neat polymer to ArG1 and ArG2 blends, modulus and stress at break slowly decreases and, only in ArG3 composition, a considerable plasticizing effect is observable, in accordance with the hypothesis previously suggested.

3.9. Scanning electron microscopy (SEM) of ApG and of ArG blends

The micrographs of ApG1 (Fig. 11) and ArG1 (Fig. 12) fracture surfaces are hereafter reported.

The ApG1 micrograph (Fig. 11) shows a tracked and smoothed surface, where it is possible to observe zones of

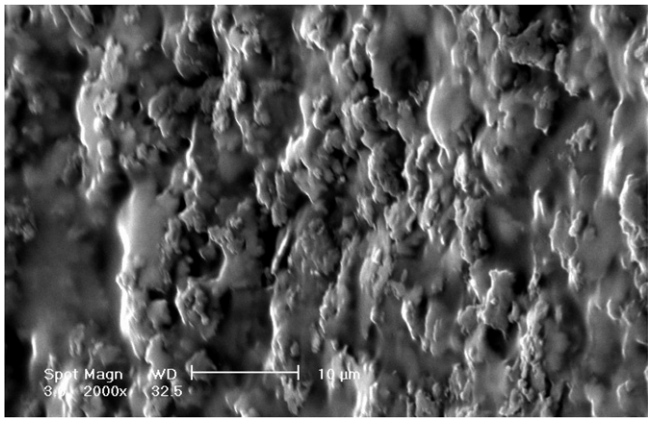

Fig. 11. SEM micrograph of ApG1 blend fracture surface.

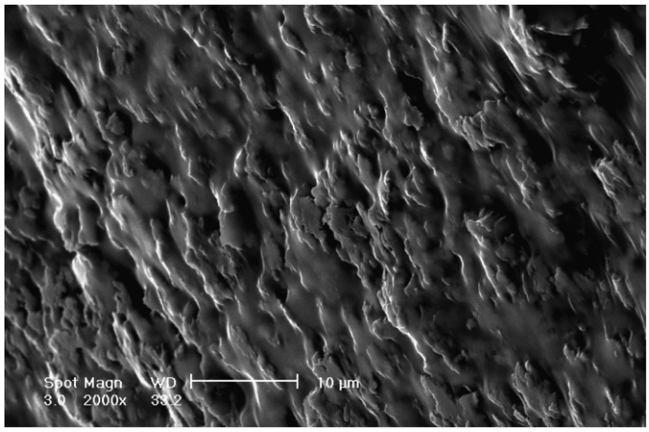

Fig. 12. SEM micrograph of ArG1 blend fracture surface.

higher material agglomeration, typical of an induced plasticizing effect, as confirmed by mechanical and thermal properties.

The ArG1 micrograph (Fig. 12) shows an indented and tracked surface, with an homogeneous distribution of material; this micrograph does not provide evident information of a plasticizing process, in accord with experimental performed data.

4. Conclusions

From the above results the following conclusions may be obtained. The plasticizing effect of glycerol on two alginates different for molecular weight and microstructure is effectively regulated by mass ratios between the polymers and the glycerol. The properties of blends are strongly related to the molecular structure of the polysaccharides used; in particular high guluronate residues content and high molecular weight represent the correct compromise of microstructural properties able to allow to the glycerol molecules to be entangled in specific binding sites of the polymeric network, whereas lower molecular weight and higher content of mannuronate residues give rise to a flexible, linear three-dimensional arrangement scarcely interacting with the plasticizer introduced; only at high concentration of glycerol, in fact, it is possible to observe a slight interaction of the glycerol itself with the intermolecular binding sites.

As concerning the potential applications of the films obtained, our research is targeted to the preparation of Ap based formulations to be tested on the soil as mulching coatings. For this particular purpose the choice of Ap alginate seems to be more reasonable in view of the mechanical behaviour and of the possibility to tune them with glycerol. In fact, although the recorded mechanical properties of the obtained films are lower if faced with those ones reported for starch based films, nevertheless we must consider that the proposed application of our formulations is substantially different from the application of traditional pre-formed films; in fact the spray methodology does not produce a self-standing film, but a coating supported by the underneath soil. To this aim, work is now in progress.

As a further concluding remark we wish to stress that existing starch based material for the production of mulching films needs to be thermally treated and additivated with synthetic polymers in order to process them in blowing apparatuses, with resulting high process cost. By following our approach the polysaccharides are used as they occur in nature potentially allowing in this way a significant reduction of production costs.

Acknowledgements

The authors gratefully acknowledge the fundamental financial support of the project "Biodegradable Coverages for Sustainable Agriculture," Life Environment 03/377, approved by the European Community. Thanks to Dr. Claudia Kummerloewe (Fachhochschule Osnabrueck, Germany) for assistance in Size Exclusion Chromatography analysis and Mr. Gennaro Romano (ICTP) and Mr. Giuseppe Narciso (ICTP) for great contribute in DMTA and SEM analysis, respectively.

References

Atkins, E. D. T. (Ed.). (1985). *Polysaccharides: Topics in structure and morphology*. Weinheim: VCH Verlag.

Atkins, E. D. T., Nieduszynsky, W. M., Parker, K. D., & Smolko, E. E. (1973a). Structural components of alginic acid. II. Crystalline structure of poly α-L-guluronic acid. Results of X-ray diffraction and polarized infrared studies. *Biopolymers, 12*, 1879–1887.

Atkins, E. D. T., Nieduszynsky, W. M., Parker, K. D., & Smolko, E. E. (1973b). Structural components of alginic acid. I. Crystalline structure of poly -β-D-guluronic acid. Results of X-ray diffraction and polarized infrared studies. *Biopolymers, 12*, 1865–1878.

Borchard, W., Kenning, A., Kapp, A., & Mayer, C. (2005). Phase diagram of the system sodium alginate/water. A model for biofilm. *International Journal of Macromolecules, 35*, 247–256.

Briassoulis, D. (2006a). Mechanical behaviour of biodegradable agricultural films under real field conditions. *Polymer Degradation and Stability, 91*, 1256–1272.

Briassoulis, D. (2006b). Mechanical performance and design criteria of biodegradable low-tunnel films. *Journal of Polymers and the Environment, 14*(3), 289–307.

Clark, A. H., & Ross-Murphy, S. B. (1987). Structural and mechanical properties of biopolymers gels. *Advances in Polymer Science, 83*, 57–192.

De Prisco, N., Immirzi, B., Malinconico, M., Mormile, P., Petti, L., & Gatta, G. (2002). Optical analysis of polyvinyl-alcohol-based films suitable for protected cultivation. *Journal of Applied Polymer Science, 86*, 622–632.

Draget, K. I., Smidsrød, O., & Skjak-Braek, G. (2002). Alginates from algae. *Biopolymers, 6*, 215–244.

Fischer, F. G., & Dorfel, H. (1955). Polyuronic acids in brown algae. *Z. Physiol. Chem, 302*(4–6), 186–203.

Grant, G. T., Morris, E. R., Rees, D. A., Smith, P. J. C., & Thom, D. (1973). Biological interaction between polysaccharides and divalent cations: the egg-box model. *FEBS Letters, 32*, 195–198.

Grasdalen, H. (1983). High field ^{1}H-NMR spectroscopy of alginates: sequential structure and linkage conformations. *Carbohydrates Research, 118*, 255–260.

Grasdalen, H., Larsen, B., & Smidrod, O. (1979). A P.M.R study of the composition and sequence of uronate residues in alginate. *Carbohydrates Research, 68*, 23–31.

Grasdalen, H., Larsen, B., & Smidrod, O. (1981). ^{13}C-NMR studies of monomeric composition and sequence in alginate. *Carbohydrates Research, 89*, 179–191.

Haly, A. R., & Snaith, J. W. (1971). Calorimetry of rat tail tendon collagen before and after denaturation. Heat of fusion of its absorbed water. *Biopolymers, 10*, 1681–1699.

Haug, A., Larsen, B., & Smidsrod, O. (1966). A study of the constitution of alginic acid by partial acid hydrolysis. *Acta Chemica Scandinavica, 20*, 183–190.

Heyraud, A. G. C., Leonard, C., Rochas, C., Girond, S., & Kloareg, B. (1996). NMR spectroscopy analysis of oligoguluronates and oligomannuronates prepared by acid or enzymic hydrolysis of homopolymeric blocks of alginic acid. Application to the determination of the substrate specificity of *Haliotis tuberculata* alginate lyase. *Carbohydrate Research, 289*, 11–23.

Immirzi, B., Malinconico, M., Romano, G., Russo, R., & Santagata, G. (2003). Biodegradable films of natural polysaccharides blends. *Journal of Material Science Letters, 22*(20), 1389–1392.

Nakamura, K., Nishimura, Y., Hatakeyama, T., & Hatakeyama, H. (1995). Thermal properties of water insoluble alginate films containing di- and trivalent cations. *Thermochimica Acta, 267*, 343–353.

Russo, R., Giuliani, A., Immirzi, B., Malinconico, M., & Romano, G. (2004). Macromolecular Symposia 218 (Current Topics in Polymer Science and Technology). In Alginate/polyvinyl alcohol blends for agricultural applications: Structure–properties correlation, mechanical properties and greenhouse effect evaluation, pp. 241–250.

Russo, R., Malinconico, M., Petti, L., & Romano, G. (2005). Physical behaviour of biodegradable alginate-poly(vinylalcohol) blend films. *Journal of Polymer Science, 43*, 1205–1213.

Schettini, E., Vox, G., Malinconico, M., Immirzi, B., & Santagata, G. (2005). Physical properties of innovative biodegradable spray coating for soil mulching in greenhouse cultivation. *Acta Horticulture, 691* ISHS.

Seon, J. K., Seoung, G. Y., & Sun, I. K. (2003). Synthesis and characteristics of interpenetrating polymer network hydrogels composed of alginate and poly(diallydimethylammonium chloride). *Journal of Applied Polymer Science, 91*, 3705–3709.

Smidsrod, O., Haug, A., & Larsen, B. (1966). The influence of pH on the rate of hydrolysis of acidic polysaccharides. *Acta Chemica Scandinavica, 20*(4), 1026–1034.

Standard test method for determining the chemical composition and sequence in alginate by proton nuclear magnetic resonance (^{1}H NMR) spectroscopy designation: F 2259-03, 2003.